

Agata Dudek*, Magdalena Klimas

Czestochowa University of Technology, Faculty of Processing and Material Engineering and Applied Physics

Institute of Material Engineering, al. Armii Krajowej 19, 42-200 Częstochowa, Poland

*Corresponding author: E-mail: dudek@wip.pcz.pl

Received (Otrzymano) 10.05.2013

THE MICROSTRUCTURE AND SELECTED PROPERTIES OF TITANIUM - HYDROXYAPATITE COMPOSITES OBTAINED BY SPARK PLASMA SINTERING (SPS METHOD)

Titanium implants are characterized by improved mechanical properties compared to human bones, that might lead to overtaking the whole load from the bone, which is conducive to bone resorption. One of the proposals to solve this problem is the use of composite materials based on a titanium matrix or titanium alloy matrix with an addition of hydroxyapatite (HAp) ceramics. The introduction of HAp to the metallic material contributes to improvement in biocompatibility and allows for integration of the implant with bone tissue.

The focus of this study is on examining metallic-ceramic composites based on a titanium matrix or titanium alloy matrix with an addition of hydroxyapatite ceramics HAp ($\text{Ca}_{10}(\text{PO}_4)_6(\text{OH})_2$) ranging from 20 to 40 wt.%, obtained by means of the spark plasma sintering method in the atmosphere of shield gas (argon), at the sintering temperature of 1000°C in SPS HP 5 equipment (manufactured by FCT). The samples were sintered for 25 minutes at the compaction pressure of 35 MPa. The composites were evaluated by means of structural analysis in microstructural examinations with an optical microscope, Neophot 32, and X-ray quality analysis using an X-ray diffractometer (Seifert 3003 T-T) and the following parameters: supply voltage -30 kV, current intensity -40 mA, measurement step 0.1°, integration time 10 s, characteristic radiation wavelength $\lambda_{\text{Co}} = 1.790$ nm. The hydrostatic weighing method in deionized water according to standard PN-EN ISO 2738: 2001 was used to measure the density, porosity and water absorption. The surface profile of the biocomposites was determined using a Hommel T1000 roughness tester. The roughness parameters were measured in contact with the examined surface by coupling the stylus with a differential measurement system. The mechanical properties (hardness) of the metallic-ceramic composites based on a titanium matrix or titanium alloy matrix with an addition of hydroxyapatite ceramics HAp were evaluated. The aim of the study was to determine the usefulness of the SPS (Spark Plasma Sintering) method for manufacturing metallic-ceramic composites for medical applications.

Keywords: SPS method, metallic-ceramic composites, titanium, hydroxyapatite

MIKROSTRUKTURA I WYBRANE WŁAŚCIWOŚCI KOMPOZYTÓW TYTAN - HYDROKSYAPATYT OTRZYMYWANYCH METODĄ ISKROWEGO SPIEKANIA PLAZMOWEGO (METODA SPS)

Implanty tytanowe charakteryzują się wysokimi w porównaniu z kośćmi właściwościami mechanicznymi, może to prowadzić do przejścia całości obciążeń, sprzyjając tym samym resorpcji kości. Jedną z propozycji rozwiązania tego problemu są materiały kompozytowe na osnowie tytanu i stopu tytanu z dodatkiem ceramiki hydroksyapatytowej. Wprowadzenie cząsteczek HAp do materiału metalicznego przyczynia się do zwiększenia biogodności, jak również umożliwia tworzenie wiązań pomiędzy implantem a tkanką kostną.

Przedmiotem badań przedstawionych w niniejszym artykule są kompozyty metaliczno-ceramiczne na osnowie tytanu lub stopu tytanu z dodatkiem ceramiki hydroksyapatytowej HAp ($\text{Ca}_{10}(\text{PO}_4)_6(\text{OH})_2$) od 20 do 40% wagowych otrzymane metodą iskrowego spiekania plazmowego (spark plasma sintering) w atmosferze gazu ochronnego argonu w temperaturze spiekania 1000°C w urządzeniu typu SPS HP 5 firmy FCT. Próbkę były spiekane przez czas 25 min przy ciśnieniu prasowania 35 MPa. Kompozyty poddano analizie strukturalnej, badając ich mikrostrukturę przy użyciu mikroskopu optycznego Neophot 32, oraz rentgenowskiej analizie jakościowej, stosując dyfraktometr rentgenowski Seifert 3003 T-T przy następujących parametrach: napięcie zasilające -30 kV, natężenie prądu -40 mA, krok pomiarowy 0,1°, czas zliczania 10 s, długość fali promieniowania charakterystycznego $\lambda_{\text{Co}} = 1,790$ nm. Oceniono gęstość, porowatość oraz nasiąkliwość otrzymanych kompozytów metodą ważenia hydrostatycznego w wodzie dejonizowanej, zgodnie z normą PN-EN ISO 2738: 2001. Określono ponadto topografię powierzchni biokompozytów, stosując do tego celu profilometr Hommel T1000. Wyznaczenie parametrów chropowatości powierzchni wykonano w kontakcie z badaną powierzchnią przez sprzężenie igły z różnicowym układem pomiarowym. Oceniono właściwości mechaniczne (mikrotwardość) otrzymanych kompozytów metaliczno-ceramiczne na osnowie tytanu lub stopu tytanu z dodatkiem ceramiki hydroksyapatytowej HAp. Celem badań było określenie przydatności metody iskrowego spiekania plazmowego (spark plasma sintering) do wytwarzania kompozytów metaliczno-ceramicznych do zastosowań medycznych.

Słowa kluczowe: metoda SPS, kompozyty metaliczno-ceramiczne, tytan, hydroksyapatyt

INTRODUCTION

The most popular metal employed in bone surgery is titanium and its alloys. Titanium implants are characterized by improved mechanical properties compared to human bones, that might lead to overtaking the whole load from the bone, which is conducive to bone resorption. One of the proposals to solve this problem is the use of composite materials based on a titanium matrix and titanium alloy matrix with an addition of hydroxyapatite (HAp) ceramics. The introduction of HAp to the metallic material contributes to improvement in biocompatibility and allows for integration of the implant with bone tissue [1-5].

The method of spark plasma sintering is one of the most modern methods of powder sintering [4-6]. The factors which distinguish this method from conventional methods include a lower temperature during the sintering process and lower pressure during compaction [6]. The method helps shorten the sintering time due to impulse-based heating that reduces the activation energy of diffusion processes, which causes the microstructure of the obtained parts to remain unchanged and grain grown is observed during heat treatment [4, 6, 7]. Furthermore, the SPS method does not necessitate initial compaction, isostatic pressing or drying. The materials obtained with this method are characterized by a uniform and homogeneous structure across the sinter volume [8, 9]. Impulses of direct current are used for heating the sintered materials, which adds a quasi-adiabatic character to the heating process, thus ensuring -high thermal effectiveness. Heat is ensured by Joule's effect. There are two methods of current flow: through stamps and a graphite die or through compacted powder grains. Current flow through compacted powder grains occurs as a result of arc discharge in the pores between the compressed powder particles, tunnelling through the layer of oxides on the powder surface at the location of their contact or electrical avalanche breakdown [10]. When the current flows through the powder, a spark discharge occurs at the contact points and removes gases and oxides adsorbed from the particle surfaces. The resultant vapour is converted to the plasma state. The mechanisms of mass transport in the method of spark plasma sintering are similar to conventional methods (evaporation, condensation, surface diffusion, volume diffusion and grain boundary diffusion) but they occur at a considerably higher intensity [11, 12]. The method of spark plasma sintering allows for sintering of any types of powders that conduct electricity or any mixtures of powders. The only condition that has to be met by the sintered materials is good conductivity [13].

MATERIAL

In order to obtain metallic-ceramic composites, the authors used hydroxyapatite (HAp) powders ($\text{Ca}_{10}(\text{PO}_4)_6(\text{OH})_2$) with a mean grain size of $17.89 \mu\text{m}$,

titanium alloy Ti6Al4V with a mean chord length of $14.57 \mu\text{m}$ and titanium with a mean chord length of $31.50 \mu\text{m}$. The powders were homogenized and then the mixtures of the respective powders (see Tab. 1) were placed in the matrix with a diameter of 20 mm with two stamps. A graphite foil, Papyex N998, was placed between the powder, matrix and stamps for technological purposes.

TABLE 1. Composites obtained in the study
TABELA 1. Zestawienie wytworzonych kompozytów

Specimen No.	Specimen type
1	80% Ti + 20% HAp
2	80% Ti6Al4V + 20% HAp
3	60% Ti6Al4V + 40% HAp

The composites were obtained by means of spark plasma sintering in the atmosphere of shield gas (argon) in SPS HP 5 equipment (manufactured by FCT). Table 2 presents the parameters of the heat treatment used in the study.

TABLE 2. Parameters of composite sintering
TABELA 2. Parametry spiekania kompozytów

Parameter	Sintering temperature	Sintering time	Heating rate	Compaction pressure	Impulse duration	Interval between impulses
Value	1000°C	25 min	200°C/min	35 MPa	40 ms	10 ms

RESULTS

The composites obtained by means of spark plasma sintering were then used in microstructural examinations with an optical microscope, Neophot 32. The microstructures obtained for individual composites are presented in Figures 1 to 3.

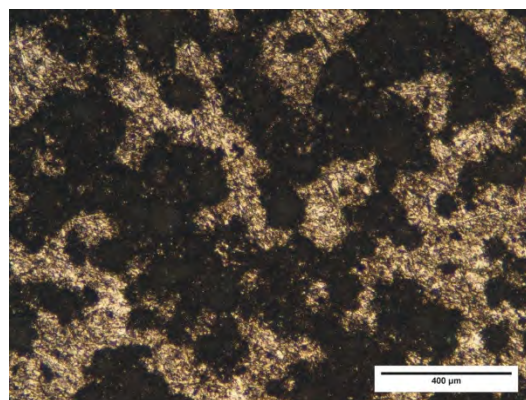


Fig. 1. Microstructure of 80% Ti + 20% HAp composite

Rys. 1. Mikrostruktura próbki kompozytu 80% Ti + 20% HAp

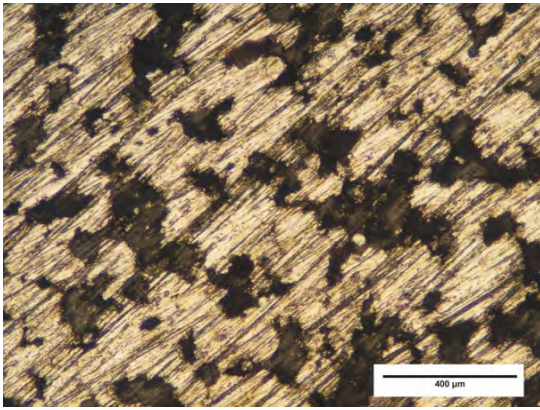


Fig. 2. Microstructure of 80% Ti6Al4V + 20% HAp composite
Rys. 2. Mikrostruktura próbki kompozytu 80% Ti6Al4V + 20% HAp

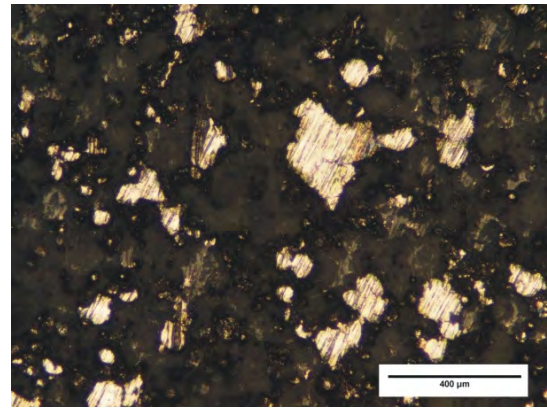


Fig. 3. Microstructure of 60% Ti6Al4V + 40% HAp composite
Rys. 3. Mikrostruktura próbki kompozytu 60% Ti6Al4V + 40% HAp

Observation of the structures of the obtained composites revealed the presence of a ceramic phase (hydroxyapatite, dark fields) and metallic phase (titanium, light fields). Additionally, pores are also represented by dark fields. The presence of pores and a higher content of hydroxyapatite in the specimen of the 60% Ti6Al4V + 40% HAp composite explains the rapid increase in dark fields observed in the microstructure of this specimen compared to the microstructure of the 80% Ti6Al4V + 20% HAp composite.

The temperature causes the hydroxyapatite ceramics to decompose, which affects its biodegradation and biotolerance in human body fluids. In order to determine phase the composition of the obtained composites, the authors carried out X-ray phase analysis using an X-ray diffractometer (Seifert 3003 T-T) and the following parameters: supply voltage -30 kV, current intensity - 40 mA, measurement step 0.1° , integration time 10 s and characteristic radiation wavelength $\lambda_{Co} = 1.790$ nm. The diffractograms obtained in the study are presented in Figure 4.

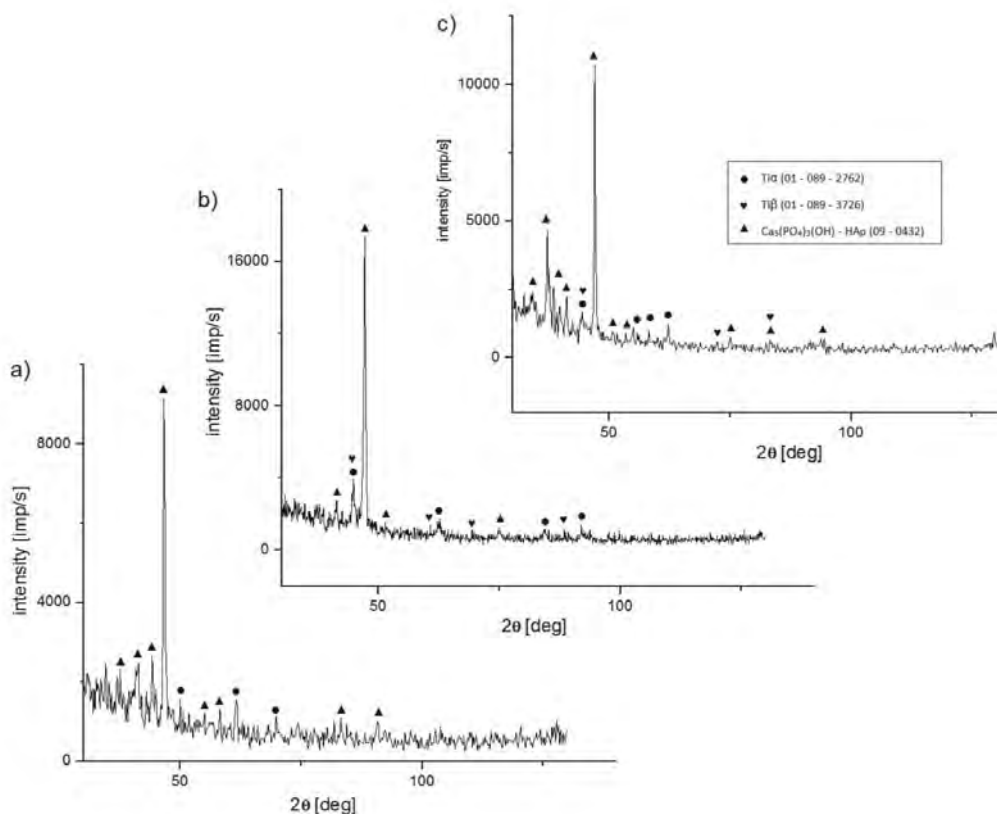


Fig. 4. Diffractograms of composites: a) 80% Ti + 20% HAp, b) 80% Ti6Al4V + 20% HAp, c) 60% Ti6Al4V + 40% HAp
Rys. 4. Dyfraktogram kompozytu: a) 80% Ti + 20% HAp, b) 80% Ti6Al4V + 20% HAp, c) 60% Ti6Al4V + 40% HAp

The reflections for the hydroxyapatite phase with a hexagonal lattice were found in the diffractograms. They had the following cell parameters: $a = b = 9.418 \text{ \AA}$, $c = 6.884 \text{ \AA}$ with space group P63/m, peaks from the Ti α phase which crystallized in the hexagonal lattice with cell parameters: $a = 2.951 \text{ \AA}$, $b = 2.951 \text{ \AA}$, $c = 4.644 \text{ \AA}$, $\alpha = 90^\circ$, $\beta = 90^\circ$, $\gamma = 120^\circ$ and in space group P63/mmc and peaks from the Ti β phase that crystallizes in the cubic lattice with cell parameters $a = b = 2.867 \text{ \AA}$, $c = 3.311 \text{ \AA}$, $\alpha = \beta = \gamma = 90^\circ$ and space group Im-3m. The density (Figs. 5, 6), porosity (Figs. 7, 8) and water absorption (Fig. 9) in the obtained composites were measured by means of the method of hydrostatic weighing in deionized water according to standard PN-EN ISO 2738: 2001. Then the samples were washed and dried. The measurements were carried out with an accuracy of 0.01 g for 3 specimens of each composite.

The obtained values of apparent density of the 80%Ti+20%HAp and 80%Ti6Al4V+20%HAp composites result from the differences in the content of metallic powders used and improved thickening of the HAp and Ti6Al4V powders with a comparable grain size.

The increase in hydroxyapatite addition up to the content of 40% caused a decrease in apparent density to the level of 3.61 g/cm^3 . The addition of hydroxyapatite ceramics caused a decrease in the relative density of the composites, connected with an increasing total porosity (Fig. 8).

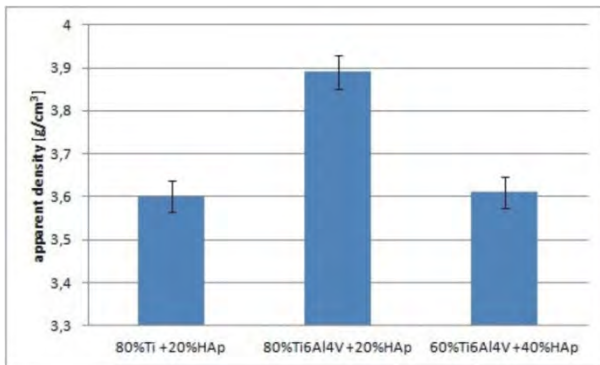


Fig. 5. Apparent density of metallic-ceramic sinters

Rys. 5. Gęstość pozorna spieków metaliczno-ceramicznych

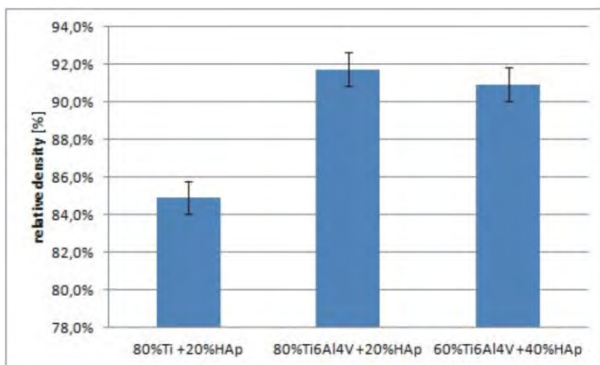


Fig. 6. Relative density of metallic-ceramic sinters

Rys. 6. Gęstość względna spieków metaliczno-ceramicznych

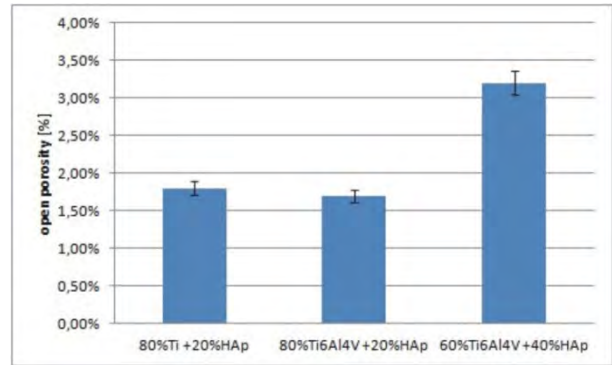


Fig. 7. Open porosity of metallic-ceramic sinters

Rys. 7. Porowatość otwarta spieków metaliczno-ceramicznych

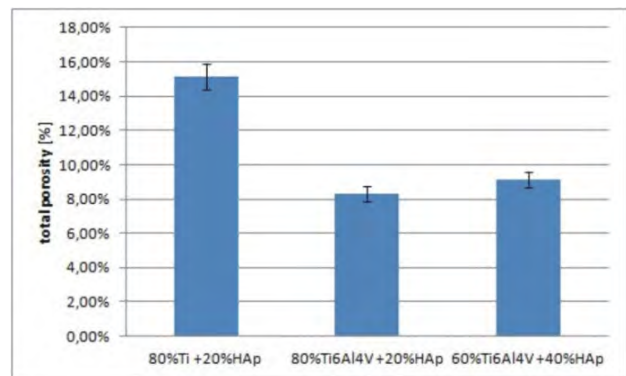


Fig. 8. Total porosity of metallic-ceramic sinters

Rys. 8. Porowatość całkowita spieków metaliczno-ceramicznych

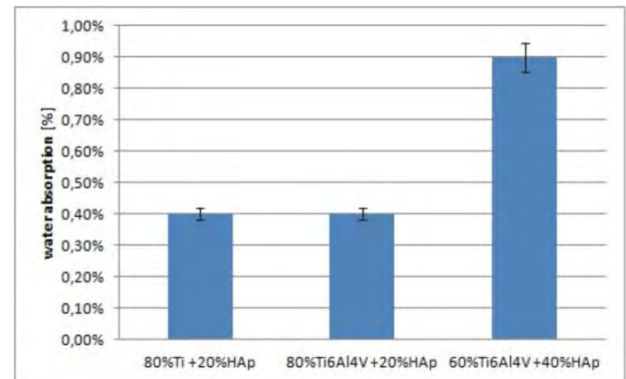


Fig. 9. Water absorption of metallic-ceramic sinters

Rys. 9. Nasiąkliwość spieków metaliczno-ceramicznych

Analysis of the results obtained for porosity measurements revealed that the open porosity of the composites based on a titanium matrix and titanium alloy Ti6Al4V with the same content of hydroxyapatite was comparable. An increase in open porosity was observed in the specimen containing 40% HAp compared to the specimen with 20% HAp. A higher total porosity was observed for the titanium-matrix composite compared to the composite based on the titanium alloy Ti6Al4V matrix, which correlates with the density measurements for the studied composites. An increase in hydroxyapatite content causes a rise in total porosity. The porosity obtained by means of hydrostatic weighing was con-

firmed by microstructural analysis of the studied materials. It should be noted that the mean grain size of the titanium powder was nearly twice higher compared to the Ti6Al4V powder, which affected the degree of powder compaction (packing) of individual particles within the whole sinter.

The results obtained for water absorption of the metallic-ceramic composites should be analysed together with the results obtained for open porosity in individual sinters. The highest water absorption among the materials used was found in the composite with a 40% addition of ceramic phase.

In order to determine the surface profile parameters, the authors used a Hommel T1000 roughness tester. The roughness parameters were measured in contact with the examined surface by coupling the stylus with a differential measurement system.

The results represented by arithmetic means from three measurements for each sample are shown in Table 3.

TABLE 3. Roughness parameters measured on specimen surface

TABELA 3. Zestawienie parametrów chropowatości powierzchni próbek

Specimen	Parameter					
	R_t [μm]	R_{max} [μm]	R_z [μm]	R_a [μm]	R_p [μm]	RSm [mm]
80% Ti + 20% HAp	24.64	24.64	18.20	3.65	4.35	0.1000
80% Ti6Al4V + 20% HAp	7.34	7.05	4.55	0.73	1.44	0.0800
60% Ti6Al4V + 40% HAp	17.94	15.97	12.31	1.68	5.14	0.0597

R_t - total height of profile

R_{max} - maximum deviation

R_t - maximum height of profile

R_a - arithmetic mean of profile ordinates

R_p - maximum peak height

RSm - average width of valleys in profile elements

The highest value of mean arithmetic deviation of the profile ordinates from the mean line, termed the R_a parameter, was observed for the specimen with a titanium matrix containing 20% HAp. The sudden decline in the R_a parameter in the specimen with the titanium alloy matrix compared to the specimen with the titanium matrix with the same HAp content is connected with the grain size of the powders used to obtain the composites. The smaller the powder grains, the lower surface roughness of the obtained material. The surface roughness in materials for medical applications is decisive in osseointegration between the implant and bone. A higher roughness in the material surface promotes the adsorption of proteins and faster osseointegration, which has been demonstrated in the study [11].

In order to determine the strength properties of the obtained metallic-ceramic composites, the authors examined the microhardness by means of the Microhardness Tester FM-7 with a Vickers indenter with the

load of 100 G. The hardness of the composites is presented in the form of a chart (see Figure 10).

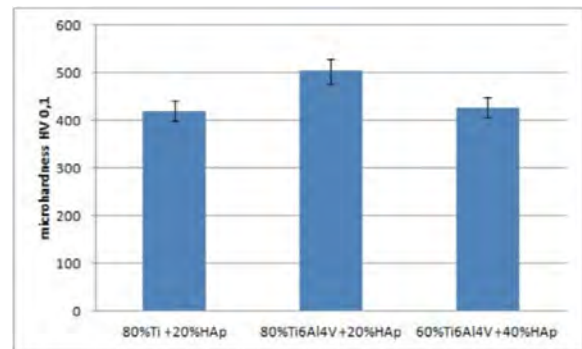


Fig. 10. Microhardness of metallic-ceramic composites

Rys. 10. Wykres mikrotwardości kompozytów metaliczno-ceramicznych

The highest microhardness was obtained for the sinter with the titanium Ti6Al4V matrix with the addition of 20% HAp (503.26 HV0.1). The increase in hydroxyapatite addition causes a reduction in microhardness to the value of 427.68 HV0.1. As for the specimens with the same content of hydroxyapatite, a higher microhardness is observed in the composite with the Ti6Al4V titanium alloy matrix compared to the composite with pure titanium, which exhibits a lower apparent density and higher total porosity.

CONCLUSION

The microstructural analysis of the metallic-ceramic composites showed that the addition of bioactive hydroxyapatite ceramics to Ti and Ti6Al4V powders results in increased open porosity and total porosity in the composites obtained by means of the SPS method, which directly affects water absorption in the obtained materials and which, in the context of their application in implantology, seems to be of much interest and a highly desirable outcome. When attempting to achieve optimum (from the standpoint of application of the composites) values of roughness parameters, one should note that the addition of a hydroxyapatite phase to composites based on a titanium alloy causes an increase in surface roughness observed in the obtained materials.

The parameters used during the process of sintering did not cause decomposition of the hydroxyapatite. Furthermore, it should be noted that the results obtained for the total porosity of the composites are affected by the grain size and types of grains in the metallic powder.

The results of the measurements of hardness in the materials obtained by means of the SPS method confirmed the changes observed in the material structure and correlate with the results obtained for the relative density of these materials.

The findings of this study seem to be promising with regard to the prospective application of the obtained composites in implantology.

REFERENCES

- [1] Kim Y.H., Koak J.Y., Chang I.T., Wennerberg A., Heo S.J., A histomorphometric analysis of the effects of various surface treatment methods on osseointegration. *Int. J. Oral Maxillofac. Implants* 2003, 18, 349-356.
- [2] Thian E.S., Loh N.M., Khor K.A., Tor S.B., Ti6Al4V/HAp composite feedstock for injection molding, *Materials Letters* 2002, 56, 522-532.
- [3] Dudek A., *Kształowanie własności użytkowych biomateriałów metalicznych i ceramicznych*, Wyd. Politechniki Częstochowskiej, Częstochowa 2010.
- [4] Mondal D., Nguyen L., Oh I.-H., Lee B.-T., Microstructure and biocompatibility of composite biomaterials fabricated from titanium and tricalcium phosphate by spark plasma sintering, *J. Biomed. Mater. Res.* 2013, Part A, 101A, 1489-1501.
- [5] Klimas M., Dudek A., Method of obtaining metallic-ceramic composites of Ti + HAp and its effect on structural properties, *Engineering of Biomaterials* 2012, 15, 116-117, 48-51.
- [6] Anawati, Tanigawa H., Asoh H., Ohno T., Kubota M., Ono S., Electrochemical corrosion and bioactivity of titanium - hydroxyapatite composites prepared by spark plasmasintering, *Corosion Science* 2013, 70, 212-220.
- [7] Garbiec D., Rybak T., Heyduk F., Janczak M., Nowoczesne urządzenie do iskrowego spiekania plazmowego proszków SPS HP D 25 w Instytucie Obróbki Plastycznej, *Obróbka Plastyczna Metali* 2011, t. XXII, 3.
- [8] Nygren M., Shen Z., On the preparation of bio-, nano- and structural ceramics and composites by spark plasma sintering, *Solid State Sciences* 2003, 5, 125-131.
- [9] Nishimura T., Mitomo M., Hirotsuru H., Kawahara M., Fabrication of silicon nitride nano-ceramics by spark plasma sintering, *Journal of Materials Science Letters* 1995, 1046-1047.
- [10] A., Oleszak D., Rosiński M., Nanokrystaliczne kompozyty NiAl-TiC spiekane metodą impulsowo-plazmową, *Inżynieria Materiałowa* 2004, 5(142), 820-823.
- [11] Michalski A., Rosiński M., Metoda impulsowo-plazmowego spiekania: podstawy i zastosowanie, *Inżynieria Materiałowa* 2010, t. XXXI, 1, 7-11.
- [12] <http://www.ios.krakow.pl/282,a,spiekanie-metoda-sps.htm> - marzec 2013.
- [13] Garbiec D., Rybak T., Heyduk F., Spiekanie tytanu i hydroksyapatytu metodą iskrowego spiekania plazmowego, *Hutnik-Wiadomości Hutnicze* 2012, 8, 569-574.
- [14] Dobedoe R.S., West G.D., Lewis M.H., Spark plasma sintering of ceramics, *Bulletin of the European Ceramic Society* 2003, 1, 19-24.